JOURNAL OF GUIDANCE, CONTROL, AND DYNAMICS
Vol. 33, No. 3, May–June 2010

Optimal Control of Gravity-Tractor Spacecraft for Asteroid Deflection

Joris T. Olympio*
ESA, 2200 AG Noordwijk, The Netherlands

DOI: 10.2514/1.46378

Near-Earth objects can pose a major threat to Earth. New ideas and concepts are continually proposed to mitigate possible impact. Among them, the gravity tractor is promising and has been the focus of many recent studies on asteroid deflection. The gravity-tractor concept is studied and trajectories are designed to lessen the risk of impact of a near-Earth object. By means of a mathematical model of the gravity tractor, a high-fidelity trajectory design method for deflection is proposed. The optimal deflection of an asteroid is computed by an indirect method, and the trajectory of the spacecraft is deduced by an inversion of dynamics and optimal control. When the deflection achieved is compared with results published to date, the better performance of the deflection is clear. This paper shows that current literature analyses of the gravity-tractor design may be nonoptimal because the assumption made about the control penalizes the concept. The use of optimal control actually improves the robustness of the designed trajectory while obtaining higher deflection.

Nomenclature

$\mathbf{A}$	=	asteroid push acceleration, m/s^2
a	=	asteroid semimajor axis, m
d	=	equilibrium distance between the asteroid and the spacecraft, m
E	=	energy
F_{th}	=	spacecraft thruster thrust amplitude, N
$\mathbf{f}$	=	dynamic equations
H	=	Hamiltonian
I_{sp}	=	spacecraft thruster specific impulse, s
m_f	=	spacecraft dry mass, kg
m	=	mass, kg
r	=	asteroid radius, m
$\mathbf{r}$	=	heliocentric position, m
T	=	total spacecraft thrust force, N
t_f	=	end of deflection mission, MJD
t_s	=	potential impact date on Earth, MJD
t_0	=	start of deflection mission, MJD
$\mathbf{u}$	=	spacecraft unit control vector
$\mathbf{u}_A$	=	virtual asteroid unit control vector
$\mathbf{v}$	=	heliocentric velocity, m/s
$\mathbf{x}$	=	state vector
$\Delta\mathbf{r}$	=	spacecraft relative position to the Asteroid, m
$\Delta\mathbf{v}$	=	spacecraft relative velocity to the Asteroid, m/s
$\Delta\zeta$	=	deflection, m
$\boldsymbol{\lambda}$	=	costate vector
μ	=	gravitational parameter, m^3/s^2
ν_f	=	Lagrange scalar for constraint
$\boldsymbol{\pi}_f$	=	transversality conditions
ϕ	=	thruster cant angle, rad
ψ_f	=	terminal constraints

Subscripts

ast	=	asteroid
Earth	=	Earth
sc	=	spacecraft
sun	=	sun

Received 17 July 2009; revision received 11 January 2010; accepted for publication 19 January 2010. Copyright © 2010 by Joris Olympio. Published by the American Institute of Aeronautics and Astronautics, Inc., with permission. Copies of this paper may be made for personal or internal use, on condition that the copier pay the $10.00 per-copy fee to the Copyright Clearance Center, Inc., 222 Rosewood Drive, Danvers, MA 01923; include the code 0731-5090/10 and $10.00 in correspondence with the CCC.

*Research Fellow, Advanced Concepts Team, European Space Research and Technology Centre, Keplerlaan 1, Postbus 299. Member AIAA.

I. Introduction

NEAR-EARTH objects (NEOs) have attracted a lot of attention from astronomers in recent years. The possibility of an NEO impacting Earth, with dramatic consequences, motivates scientists and engineers to devise original and innovative ideas to disrupt or deflect asteroids. The latter option is often preferred [1]. Aside from political issues arising from deploying nuclear devices for asteroid fragmentation, disrupting an asteroid increases the risk of producing new impactors, particularly when the NEO is a porous rubble-pile asteroid. With sufficient warning time, deflection techniques are thus very attractive to avert an impact.

The gravity tractor was introduced recently by Lu and Love [2] as a possible means of asteroid deflection and asteroid impact mitigation. During close proximity of a spacecraft to an asteroid, the mutual gravitational acceleration perturbs both objects' dynamics. When the spacecraft can thrust in a direction that balances the gravitational force exerted by the asteroid on the spacecraft, the asteroid is accelerated and deviates slightly from its original path. This can eventually perturb the asteroid orbit, and in the long run will result in a significant deflection, preventing a potential impact on Earth. One of the main advantages of this thrusting deflection technique is that it is relatively independent of the physical properties of the asteroid, such as its composition, although the shape and gravity field might be more relevant [3].

The gravity-tractor concept has been the focus of many studies since it was introduced a few years ago. Most of the studies, however, make major assumptions about the deflection strategy and only focus on simple hovering control.

Wie [4] studies the gravity-tractor hovering dynamics. Some of his work also focus on the dynamics of solar sails as a gravity tractor. The concept is actually quite attractive, as the spacecraft in this case has very limited thrust requirement, although maintaining a non-Keplerian displaced orbit [5] or distant halo-type orbit, with or without solar sail for an autonomous vehicle, is not straightforward.

Fashnestock and Scheeres [3] study the control requirement for the coupled rotational and translational dynamics, in addition to the system specifications. With a rigorous model, this paper points out the difficulty of the control problem.

Broschart and Scheeres [6] study the hovering dynamics in the case of scientific observation of a small asteroid. Although the authors compute the equilibrium condition, the dynamic influence of the sun is neglected. Indeed, during inertial hovering for asteroid

surface mapping, the time of operation is too small for the sun actually to have an influence on the asteroid dynamics. Some work [7] also proposes a method to compute the hovering dynamics in the case of nonspherical asteroids.

In [8], the author performs local optimization for the gravity-tractor concept from launch to the rendezvous, to show that the gravity-tractor concept performance usually depends heavily on the design.

In this paper, the entire mission concept is studied, from the start of the deflection to the end. In particular, it is shown that current literature assumptions limit the efficiency of the gravity-tractor concept and may also lead to nonrealizable missions. On the other hand, a complete study shows that not only is the concept much more reliable than is shown in the literature, but as a mission, it is also more robust. This paper proposes an approach to optimal deflection of an asteroid with a gravity-tractor spacecraft. The approach can be split into two parts. First, the optimal deflection trajectory of the asteroid is computed, regardless of the spacecraft dynamics. In the second step, through dynamic inversion and optimal control, the spacecraft trajectory that would eventually optimally deflect the asteroid is estimated. Finally, the approach is applied to the deflection of asteroid 2007 VK184, one of the current asteroids graded 1 on the Torino scale.

II. Problem Statement

A. Analytical Deflection Formula

When potential asteroid impact is monitored, the location of the impact is plotted on a projection plane, which often corresponds to the B plane at Earth and at the time of potential impact [9]. The required deflection to avoid an impact is given by the distance from the undeflected impact point to the Earth's surface. For instance, in Fig. 1, the impact location (represented by an uncertainty ellipse because of inaccurate orbital parameters) is outside the Earth image and no impact on Earth is possible. Sometimes, however, the closest point location is not in the Earth image, but the close approach of the asteroid still leads to future impact conditions. The point of closest approach is said to be in a keyhole [9,10], which is a preimage of the Earth on the B plane, at the date of encounter, that leads to a future impact. Thus, if the asteroid passes through a keyhole, it will impact on the Earth after a resonant return.

If actions are required to mitigate a possible asteroid impact, a response is to deflect the asteroid by a given amount such that the impact point misses the Earth shadow or the keyhole. A good point about keyholes, though, is that they are usually smaller than the Earth shadow, and thus a small deflection would be sufficient to nullify the risk of impact. Izzo [11] generalizes the asteroid deflection formula:

$$\Delta\zeta = -\frac{3av_{\text{Earth}}(t_s)\sin\theta}{\mu}\int_{t_0}^{t_f}(t_s - t)[\mathbf{v}_{\text{ast}}(t)\cdot\mathbf{A}(t)]\,\mathrm{d}t \qquad (1)$$

which is used to compute the deflection achieved on the B plane defined at the date t_s. The acceleration $\mathbf{A}(t)$ can model an impact or, in our case, a continuous gravitational acceleration. This formula shows that the earlier the deflection starts, the larger the final deflection. If a direct impact is to be mitigated, $\Delta\zeta$ should be at least of one Earth radius.

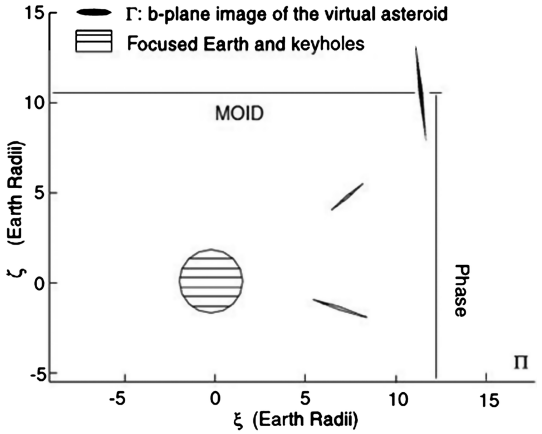

Fig. 1 ***B*** **plane and keyhole (MOID denotes the minimum orbital intersection distance).**

B. Gravity-Tractor Concept

The gravity tractor [2] uses mutual gravitational acceleration to modify the course of the asteroid with which it is in interaction. As shown in Fig. 2, the gravity-tractor spacecraft has at least two thrusters, which thrust slightly inclined in opposite directions. The thrusters are tilted, so they do not impinge the asteroid surface with ions coming from the electric propulsion system (e.g., the thrusters) and eventually reduce the efficiency of the tug system [12].

From Fig. 2, the total thrust force is then

$$T = 2F_{\text{th}}\cos\tilde{\phi} \qquad (2)$$

with $\tilde{\phi} = \sin^{-1}(\frac{r}{d}) + \phi$. The distance d must be higher than the highest dimension of the asteroid. Lu and Love [2] consider $d = 1.5r$ in the original concept. The condition for the spacecraft thrusters to compensate for the attraction of the asteroid is simply

$$\frac{T}{m_{\text{sc}}} = \frac{\mu_{\text{ast}}}{d_{\text{eq}}^2} \qquad (3)$$

A static equilibrium is then created when the spacecraft thrusts in the direction of the local gravity.

Any configuration is possible when d is chosen such that $d_{\text{eq}} \le d$, as long as there is sufficient thrust acceleration for $d_{\text{eq}} > r$. The question is only whether to have a constant or a variable relative distance d [13]. In this paper, it is assumed that the thrust amplitude F_{th} is constant when the thrusters are on. This point will, however, be discussed later.

The nonperfect shape of the asteroid introduces harmonics in the asteroid's gravitational potential, which might impose a nonconstant distance d_{eq} when the asteroid is rotating. For simplicity, this will not be taken into account in the present study, and the asteroid gravity model is assumed to be a homogeneous sphere.

C. General Dynamics

The gravity-tractor spacecraft evolves under the influence of the sun and the asteroid to deflect. Newtonian dynamics describing the relative motion of the spacecraft with respect to the asteroid in the supposed inertial heliocentric reference frame give

$$\mathbf{f}_{\text{sc}}(\mathbf{x}_{\text{sc}}, \mathbf{x}_{\text{ast}}, \mathbf{u}; t) = \begin{bmatrix} \Delta\mathbf{v}(t) \\ -\mu_{\text{sun}}\left(\frac{\Delta\mathbf{r}(t)+\mathbf{r}_{\text{ast}}(t)}{\|\Delta\mathbf{r}(t)+\mathbf{r}_{\text{ast}}(t)\|^3} - \frac{\mathbf{r}_{\text{ast}}(t)}{\|\mathbf{r}_{\text{ast}}(t)\|^3}\right) - \mu_{\text{ast}}\frac{\Delta\mathbf{r}(t)}{\|\Delta\mathbf{r}(t)\|^3}\left(1 + \frac{m_{\text{sc}}(t)}{m_{\text{ast}}}\right) + \frac{T}{m_{\text{sc}}(t)}\mathbf{u}(t) \\ -\frac{2F_{\text{th}}}{g_0 I_{\text{sp}}}\|\mathbf{u}(t)\| \end{bmatrix} \qquad (4)$$

with

$$\Delta\mathbf{r} = \mathbf{r}_{\text{sc}}(t) - \mathbf{r}_{\text{ast}}(t), \qquad \Delta\mathbf{v} = \mathbf{v}_{\text{sc}}(t) - \mathbf{v}_{\text{ast}}(t)$$

$$\mathbf{x}_{\text{sc}} = [\Delta\mathbf{r}, \Delta\mathbf{v}, m_{\text{sc}}]$$

One could have been tempted to use Tschauner–Hempel equations [14] instead of Eq. (4), as is done in numerous studies [10], when the

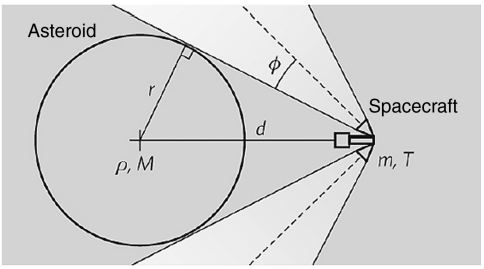

Fig. 2 Gravity-tractor concept [2].

asteroid deflected trajectory is actually not taken into account. This is a valid assumption as long as time spans are small and the effect of the towing is not studied. Indeed, when Tschauner–Hempel equations are used, the reference ellipse is an osculating ellipse of the deflected asteroid orbit that changes at all times.

Concurrently with this dynamic, the dynamic of the asteroid is considered, which is no longer given by the ephemeris, as it is being deflected by the gravity-tractor spacecraft:

$$\mathbf{f}_{\text{ast}}(\mathbf{x}_{\text{ast}}, \mathbf{x}_{\text{sc}}; t) = \begin{bmatrix} \mathbf{v}_{\text{ast}}(t) \\ -\mu_{\text{sun}} \frac{\mathbf{r}_{\text{ast}}(t)}{\|\mathbf{r}_{\text{ast}}(t)\|^3} + \mu_{\text{sc}} \frac{\Delta\mathbf{r}(t)}{\|\Delta\mathbf{r}(t)\|^3} \end{bmatrix} \tag{5}$$

Studying the motion of the center of mass of the asteroid–gravity-tractor system gives

$$\frac{\mathrm{d}^2\mathbf{r}_{\text{ast+sc}}}{\mathrm{d}t^2} + \mu_{\text{sun}} \frac{\mathbf{r}_{\text{ast+sc}}}{\|\mathbf{r}_{\text{ast+sc}}\|^3} \approx \frac{T}{m_{\text{ast}}}\mathbf{u}$$

which shows that when the spacecraft thrusts to balance the gravitational force exerted by the asteroid, the entire system is indeed accelerated [5].

D. Control Problem

Because dynamic equations (4) and (5) are highly nonlinear, finding the control $\mathbf{u}$ that would enforce a constant distance d to the asteroid during the entire mission is difficult numerically. First, the difference in scale between $\Delta\mathbf{r}$ and $\mathbf{r}_{\text{ast}}$ requires robust and accurate integrations. Second, to impose a distance d during the entire mission, state constraints must be used, which limit the solution method mostly to direct approaches. To maintain a good quality of solution, and because of the long time of flight, the number of nodes in the transcription [15] become significant. Otherwise, considering the dynamics and the constant control during a time step, the spacecraft dynamics are unlikely to respect the towing distance and, in some cases, if the thrust acceleration is not sufficient, the computation might result in the spacecraft crashing on the asteroid.

Most studies are limited to the relative motion in a circular reference frame and do not actually consider the deflection of the asteroid. Among the literature [4,6,7,16], studies related to close-proximity control and hovering above asteroids or small bodies use deadband controllers. It is apparent that to maintain a spacecraft in a prescribed relative location, deadband control provides the most straightforward approach. In this case, however, the spacecraft has to thrust while maintaining a relative distance and seeking the optimal solution.

A new approach that accurately computes both the deflected asteroid trajectory and the spacecraft control is proposed. First, the optimal deflected trajectory of the asteroid is found using an indirect method. Then from the deflected asteroid trajectory, the spacecraft trajectory is inferred. This approach is both high-fidelity and robust.

III. Optimal Deflected Asteroid Trajectory

A. Dynamic Problem of a Virtual Asteroid

A virtual asteroid is introduced with the state $\mathbf{x}_{\text{ast}} = [\tilde{\mathbf{r}}_{\text{ast}}, \tilde{\mathbf{v}}_{\text{ast}}, \tilde{m}_{\text{ast}}]$. The initial position and velocity of the virtual asteroid coincide with the position and velocity of the asteroid to deflect at one given epoch (e.g., just before the beginning of the deflection). The mass of the asteroid is also the initial gravity-tractor mass. From the general asteroid dynamic equation (5), the dynamics of our virtual asteroid are defined by

$$\tilde{\mathbf{f}}_{\text{ast}}(\mathbf{x}_{\text{ast}}, \mathbf{A}, \delta; t) = \begin{bmatrix} \tilde{\mathbf{v}}_{\text{ast}}(t) \\ -\mu_{\text{sun}} \frac{\tilde{\mathbf{r}}_{\text{ast}}(t)}{\|\tilde{\mathbf{r}}_{\text{ast}}(t)\|^3} + \delta(t)\mathbf{A}(t) \\ -\frac{2F_{\text{th}}}{g_0 I_{\text{sp}}}\delta(t) \end{bmatrix} \tag{6}$$

These dynamics define the motion of the asteroid in a central force field (e.g., sun gravitational attraction) and can be subject to a disturbing acceleration $\mathbf{A}(t)\delta(t)$. Indeed, the disturbing acceleration $\mathbf{A}(t)\delta(t)$ replaces the asteroid—spacecraft mutual gravitation acceleration in Eq. (5), although this time the spacecraft dynamics are not explicitly included. Also, $[\mathbf{A}(t), \delta(t)]$ is now the control of our virtual asteroid. The mass equation accounts for the available spacecraft fuel mass to deflect the asteroid. The optimal perturbation that a spacecraft needs to exert on the asteroid to optimally deflect it is sought.

The gentle push of the asteroid is due to the spacecraft's close proximity. Substituting Eq. (3) in Eq. (5) and comparing with Eq. (6) gives $\mathbf{A}(t)$. That being the case, this acceleration $\mathbf{A}(t)$ is bounded, and

$$\mathbf{A}(t) = \frac{T}{m_{\text{ast}}}\mathbf{u}_A \tag{7}$$

$$|\delta| \leq 1 \tag{8}$$

This constraint indicates the maximum push that the spacecraft can induce on the asteroid and thus the maximum push that our virtual asteroid can have. In addition, the mass of the virtual asteroid defines the mass of the gravity tractor. A constraint on the terminal mass is thus given by

$$\psi_f(\mathbf{x}_{\text{ast}}; t_f) = \tilde{m}_{\text{ast}}(t_f) - m_f \tag{9}$$

which limits the total amount of fuel available for the deflection.

The problem is to maximize the objective function, or performance index,

$$J = \int_{t_0}^{t_f} (t_s - t)(\mathbf{v}_{\text{ast}}(t)^T \mathbf{A}(t))\delta(t)\,\mathrm{d}t \tag{10}$$

given by the deflection equation (1), where the multiplicative term has been dropped for convenience, as it only depends on the potential impact date t_f and not on the asteroid or the spacecraft state. Parameters t_0 and t_f are thus fixed.

B. Optimal Control Problem

The optimization problem is solved using optimal control theory. Considering the dynamic equation (6) and the constraint equation (9), the control $[\mathbf{A}(t), \delta(t)]$ that maximizes the objective function J in Eq. (10) is computed.

Introducing the costate vectors $\boldsymbol{\lambda}_{\mathbf{R}}(t)$ and $\boldsymbol{\lambda}_{\mathbf{V}}(t)$ and the costate variable $\lambda_m(t)$ [assigned, respectively, to $\tilde{\mathbf{r}}_{\text{ast}}(t)$, $\tilde{\mathbf{v}}_{\text{ast}}(t)$, and $\tilde{m}_{\text{ast}}(t)$] and the constant Lagrange multiplier ν_f for the constraint ψ_f to augment the performance index, the Lagrangian is given by

$$L = J + \int_{t_0}^{t_f} \boldsymbol{\lambda}(t)^T \left(\frac{\mathrm{d}\mathbf{x}_{\text{ast}}}{\mathrm{d}t} - \tilde{\mathbf{f}}_{\text{ast}}(\mathbf{x}_{\text{ast}}, \mathbf{A}, \delta; t) \right) \mathrm{d}t + \nu_f \psi_f(\mathbf{x}_{\text{ast}}; t_f) \tag{11}$$

with $\boldsymbol{\lambda}(t)^T = [\boldsymbol{\lambda}_{\mathbf{R}}(t)^T, \boldsymbol{\lambda}_{\mathbf{V}}(t)^T, \lambda_m(t)]$.

Since the objective function is written in the Lagrange form, the Hamiltonian can be written as

$$H(\mathbf{x}_{\text{ast}}, \boldsymbol{\lambda}, \mathbf{u}; t) = (t_s - t)(\mathbf{v}_{\text{ast}}(t)^T \mathbf{A}(t))\delta(t) + \boldsymbol{\lambda}(t)^T \tilde{\mathbf{f}}_{\text{ast}}(\mathbf{x}_{\text{ast}}, \mathbf{A}, \delta; t) \tag{12}$$

The necessary conditions of optimality can be found by stating the stationarity of the Lagrangian L of the optimization problem. This leads to the well-known Euler–Lagrange equations, which describe the dynamics of the costate vectors,

$$\frac{\mathrm{d}\mathbf{x}_{\mathrm{ast}}}{\mathrm{d}t}^{T} = \frac{\partial H}{\partial \boldsymbol{\lambda}} \qquad \frac{\mathrm{d}\boldsymbol{\lambda}}{\mathrm{d}t}^{T} = -\frac{\partial H}{\partial \mathbf{x}} \tag{13}$$

and to the boundary conditions of the Euler–Lagrange equations, also called transversality conditions. For instance,

$$\boldsymbol{\pi}_f(\mathbf{x}_{\mathrm{ast}}, \boldsymbol{\lambda}; t_f) = \boldsymbol{\lambda}(t_f) - \nu_f \frac{\partial \psi}{\partial \mathbf{x_f}} \tag{14}$$

These transversality conditions provide the optimal value of $\boldsymbol{\lambda}(t_f)$. Note that $\boldsymbol{\lambda}(t_0)$ is the initial condition and is completely free. Note also that as the dynamic equations do not depend on the mass $\tilde{m}_{\mathrm{ast}}(t)$, the costate variable $\lambda_m(t)$ is constant.

Following calculus of variation theory and the maximum principle [17], the optimal control $[\mathbf{A}^*(t), \delta^*(t)]$ is the one maximizing the Hamiltonian:

$$\mathbf{u}_A^* = \arg\max_{\mathbf{u}_A} H(\mathbf{x}_{\mathrm{ast}}, \boldsymbol{\lambda}, \mathbf{A}, \delta; t)$$

and

$$H(\mathbf{x}_{\mathrm{ast}}, \boldsymbol{\lambda}, \mathbf{A}; t) = \boldsymbol{\lambda}_{\mathbf{R}}(t)^T \mathbf{r}_{\mathrm{sc}}(t) - \boldsymbol{\lambda}_{\mathbf{V}}(t)^T \frac{\mu \mathbf{r}_{\mathrm{sc}}(t)}{\|\mathbf{r}_{\mathrm{sc}}(t)\|^3} + S(\mathbf{x}_{\mathrm{ast}}, \boldsymbol{\lambda}, \mathbf{A}, \delta; t) \tag{15}$$

$$S(\mathbf{x}_{\mathrm{ast}}, \boldsymbol{\lambda}, \mathbf{A}, \delta; t) = \left(((t_s - t)\tilde{\mathbf{v}}_{\mathrm{ast}}(t) + \boldsymbol{\lambda}_{\mathbf{V}}(t))^T \mathbf{A}(t) - \lambda_m(t) \frac{2F_{\mathrm{th}}}{g_0 I_{\mathrm{sp}}} \right) \delta(t) \tag{16}$$

Clearly, the Hamiltonian is maximized for the optimal control direction:

$$\mathbf{u}_A^* = \frac{(t_s - t)\tilde{\mathbf{v}}_{\mathrm{ast}}(t) + \boldsymbol{\lambda}_{\mathbf{V}}(t)}{\|(t_s - t)\tilde{\mathbf{v}}_{\mathbf{ast}}(t) + \boldsymbol{\lambda}_{\mathbf{V}}(t)\|} \tag{17}$$

As the control belongs to a compact set ($\delta(t) \in [0, 1]$) and appears linearly in the Hamiltonian, it is in general bang–bang. In particular, S is called a switching function and is simplified to

$$S(\mathbf{x}_{\mathrm{ast}}, \boldsymbol{\lambda}, \mathbf{A}^*, \delta; t) = 2F_{\mathrm{th}} \left(\frac{\cos\tilde{\phi}}{m_{\mathrm{ast}}} \|(t_s - t)\tilde{\mathbf{v}}_{\mathbf{ast}}(t) + \boldsymbol{\lambda}_{\mathbf{V}}(t)\| - \frac{\lambda_m(t)}{g_0 I_{\mathrm{sp}}} \right) \delta(t) \tag{18}$$

This helps to choose, at each time t, whether the control $\delta(t)$ should reach its upper or lower bound ($\delta(t) = 1$ or $\delta(t) = 0$) to maximize H. Numerically, $\delta(t)$ is found by means of smoothing techniques [18].

An interesting feature of Eq. (17) is that the optimal direction of the disturbing acceleration depends on the direction of the asteroid velocity $\tilde{\mathbf{v}}_{\mathrm{ast}}$ and on how early the deflection process starts.

The optimal control is thus computed by solving a two-point boundary-value problem (TPBVP) using a shooting method. The Euler—Lagrange dynamic equations are integrated using the initial conditions $[\mathbf{x}_{\mathrm{ast}}(t_0), \boldsymbol{\lambda}(t_0)]$ while satisfying the transversality conditions $\boldsymbol{\pi}_f(\mathbf{x}_{\mathrm{ast}}, \boldsymbol{\lambda}; t_f)$ and terminal constraints $\psi_f(\mathbf{x}_{\mathrm{ast}}; t_f)$. The free vector $\boldsymbol{\lambda}(t_0)$ is used to satisfy these endpoint conditions.

C. Discussion

The optimal deflected asteroid trajectory is computed easily, and the disturbing acceleration is the spacecraft–asteroid mutual gravitational acceleration. A priori thrust phases are the phases $[\delta(t) = 1]$ in which the spacecraft is close to the asteroid and use mutual gravitation to deflect it. The coast phases $[\delta(t) = 0]$ are the phases in which the spacecraft must not perturb the asteroid dynamic. It is then very likely that the optimal way to deflect the asteroid is to alternate between thrust and coast phases. This strategy is highly dependent on the asteroid heliocentric velocity, as shown in Eq. (18). Great variation in the velocity, and thus high eccentricity of the original orbit, might lead to complex deflection control.

In many studies on the gravity tractor, the main assumption is that the spacecraft is fully thrusting, which would assume that $\delta(t) = 1$ with the present formulation. This assumption facilitates the theoretical development. But here it is clear that it is, in general, not true and that using such an assumption indeed penalizes the concept.

Such a result has many implications. For instance, from an operational point of view, coast phases are useful to reconfigure the spacecraft, correct any pointing issues, communicate with a ground base, or measure the changes so far in the asteroid's orbit. Coast arcs also make the entire mission more robust. Bearing in mind that thrusting is the critical point of such a mission, it is good to know that in case of any thrust-amplitude failure, the mission can still be recovered if there is sufficient coast time. It is known that coast phases allow more security in the thrusting [19]. Given that thrusting is the key element of the deflection strategy, coast phases are required for a fail-safe mission.

IV. Gravity-Tractor Spacecraft Trajectory

A. Inversion of Dynamics During Towing Phases

1. Position

When the spacecraft has to thrust to compensate for gravitational acceleration from the asteroid, it must be placed on the equilibrium sphere, defined by Eq. (3), and in such a position that the spacecraft thrust vector is aligned with the centers-of-mass line. The desired position of the spacecraft is thus readily computed during the towing phases. When the spacecraft is close to the asteroid, the control $\mathbf{u}_A$ is indeed the direction of the mutual gravitational acceleration. With the equilibrium condition between the thrust and the gravitational acceleration, the relative position vector is given by

$$\boldsymbol{\Delta r}(t) = \sqrt{\frac{\mu_{\mathrm{ast}} m_{\mathrm{sc}}(t)}{T\delta(t)}} \mathbf{u}_A(t) \tag{19}$$

The mass $m_{\mathrm{sc}}(t)$ of the spacecraft will slowly decrease as the spacecraft is thrusting. As mentioned in the Introduction, two options are possible.

1) Suppose a constant relative distance $\boldsymbol{\Delta} r(t) = d$, then $\phi(t)$ varies (assuming F_{th} is constant), such that the ratio

$$\frac{m_{\mathrm{sc}}(t)}{2F_{\mathrm{th}} \cos(\sin^{-1}(\frac{r}{d}) + \phi)}$$

is constant.

2) Suppose that the relative distance $\boldsymbol{\Delta} r(t) = d(t)$ varies, then Eqs. (2) and (3) give

Table 1 Property of the asteroid 2007 VK184

Epoch	2454600.5 MJD
Semi major axis a	1.726508477921687 AU
Eccentricity e	0.5698369067437545
Inclination i	1.222310015202323 deg
Argument of perihelion ω	73.0616457437701 deg
Longitude of ascending node Ω	254.0587808820642 deg
Mean anomaly M	102.686674978651 deg
Mass m_{ast}	3.3×10^9 kg
Diameter	130 m
Rotational rate	0.266 deg/day

Table 2 Date and duration of the mission

Potential impact date	17685.5 MJD (2048-06-03)
Minimum warning time	1826 days
Maximum warning time	5478 days
Maximum thrust duration	3897 days (5.3 years)

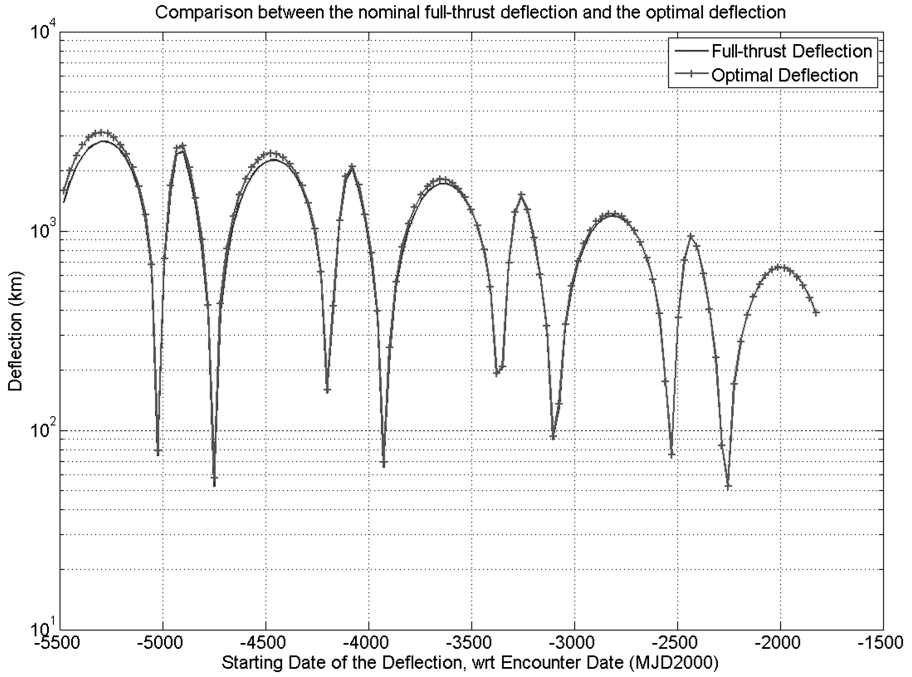

Fig. 3 Optimal and nonoptimal fully thrusting deflection with a gravity-tractor spacecraft (wrt denotes with respect to).

$$d(t)^2 - \frac{\mu_{\text{ast}} m_{\text{sc}}(t)}{2F_{\text{th}} \cos(\sin^{-1}(\frac{r}{d(t)}) + \phi)} = 0$$

which has to be satisfied.

Sanchez et al. [13] deduce that a variable-altitude hovering is less efficient than the constant-altitude option. The authors demonstrate that the constant-altitude option is more efficient by using arguments about the mass of the system, disregarding the nonlinearity of the dynamics and the optimal control contribution. However, the difference is so small that it does not seem to make a major difference. Indeed, keeping the thrust acceleration variable seems more practical, because keeping a constant altitude might be more complex, particularly for nonhomogeneous rotating asteroids. As $\delta(t)$ can be 0 or 1, the spacecraft's relative distance to the asteroid $\|\mathbf{\Delta r}(t)\|$ varies between $d_{\min}$ and infinity, where $d_{\min}$ is the distance obtained with Eq. (3) when the spacecraft has no fuel.

The mass of the spacecraft is readily computed, since the spacecraft is fully thrusting during the towing phases. To obtain the complete state of the spacecraft and compute the spacecraft's velocity during the towing phases, a dynamic inversion method is also introduced.

2. Velocity and Hovering Control

From the position and mass of the spacecraft, the spacecraft velocity during the towing phases is deduced. However, since the thrust of the spacecraft is already constrained to balance the gravitational interaction of the asteroid, one would expect the need for extra thrust acceleration to move the spacecraft into the correct position and satisfy controllability conditions.

As $\mathbf{u}_A$ is given by a continuous-function equation (17), the spacecraft position also moves continuously. Over an infinitesimal time step δt, the required additional thrust acceleration should be the difference

$$\delta\Gamma(t)\delta t \approx \frac{\mathrm{d}\mathbf{v}_{\text{sc}}}{\mathrm{d}t}(t+\delta t) - \frac{\mathrm{d}\mathbf{v}_{\text{sc}}}{\mathrm{d}t}(t)$$

The second-order differential equation in $\mathbf{r}_{\text{ast}}(t)$ [Eq. (6)], where $\mathbf{A}$ is replaced by Eqs. (8) and (19) and from which the second-order differential equation on $\mathbf{r}_{\text{sc}}(t)$ is subtracted, gives exactly

$$\frac{\mathrm{d}^2\mathbf{\Delta r}}{\mathrm{d}t^2} = -\mu_{\text{sun}}\left(\frac{\mathbf{\Delta r}(t) + \mathbf{r}_{\text{ast}}(t)}{\|\mathbf{\Delta r}(t) + \mathbf{r}_{\text{ast}}(t)\|^3} - \frac{\mathbf{r}_{\text{ast}}(t)}{\|\mathbf{r}_{\text{ast}}(t)\|^3}\right) \tag{20}$$

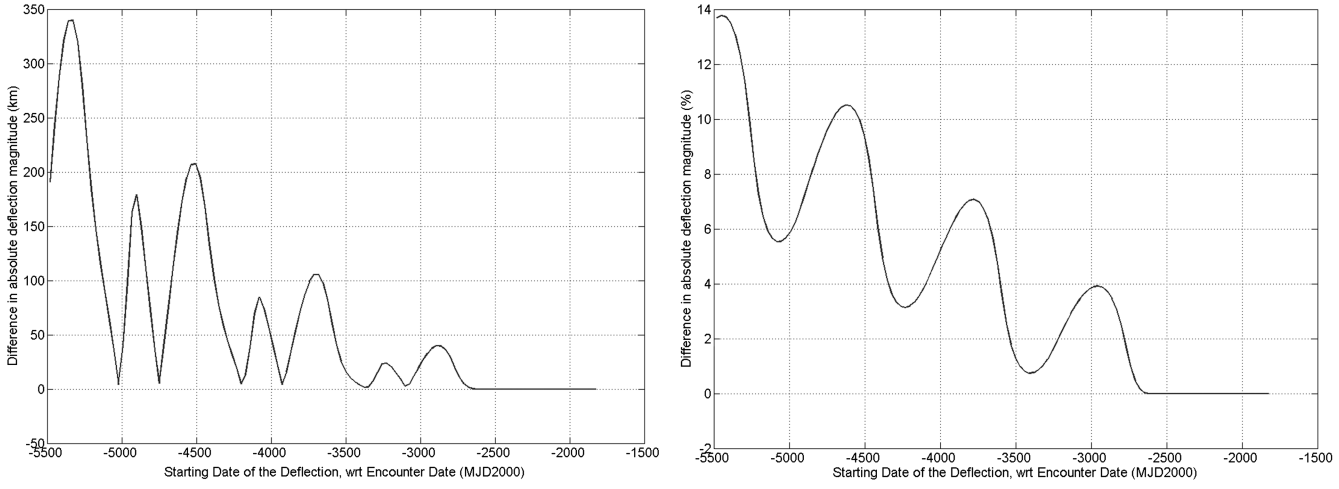

Fig. 4 Comparison of the asteroid deflection efficiency.

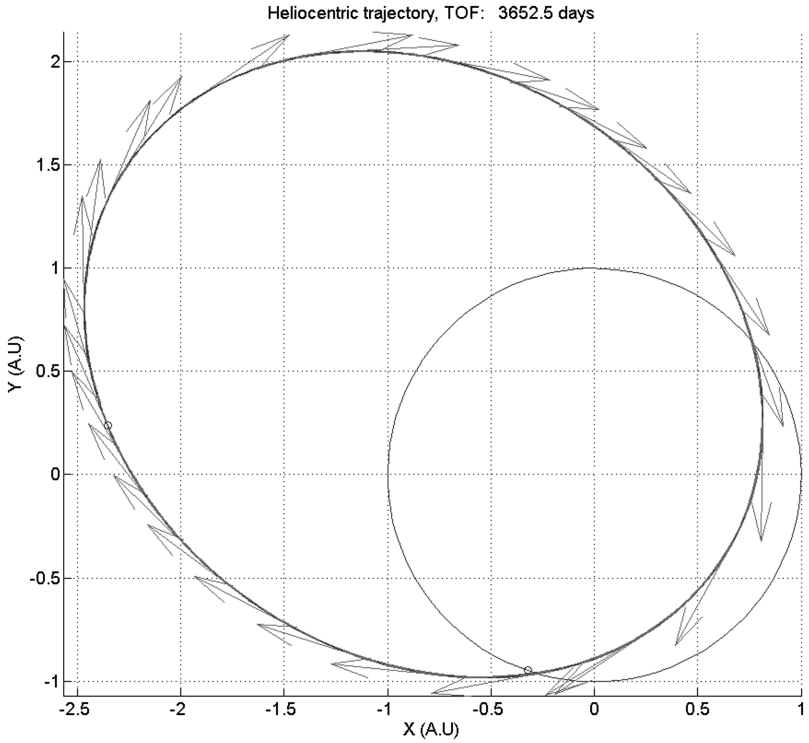

Fig. 5 Asteroid nominal and deflected trajectory (TOF denotes time of flight).

which is equivalent to Eq. (4) using the equilibrium-condition equation (3) [in a towing phase and supposing $m_{sc} \ll m_{ast}$ in Eq. (4), the terms relative to the thrust acceleration and the mutual gravitation vanish]. In other words, $\delta\Gamma = 0$. Mathematically, it shows that any C^2 functions $\mathbf{u}_A(t)$ satisfy the second-order differential equation in $\mathbf{\Delta r}$ through the equilibrium-condition equation (19) and the mutual gravitational acceleration. In addition, the regularity of $\mathbf{u}_A(t)$ is assured by the maximum principle [17], since the solution never crosses the switching curve during towing phases. Physically, this indeed confirms that the entire system that is accelerated and no additional thrust acceleration is required.

To compute $\mathbf{v}_{sc}(t)$, a collocation method [15] is used. Discretizing the time-interval into nodes $\{t_i\}$, and knowing the spacecraft position $\mathbf{\Delta r}(t_i)$ and mass $m_{sc}(t_i)$ at each node, Eq. (4) has a unique solution for each segment $[t_i,\ t_{i+1}]$ and $[t_0, t_f]$. Obviously, as the solution $\mathbf{\Delta r}(t)$ of Eq. (4) is at least C^2 [because of Eq. (19) and because $\mathbf{u}_A(t)$ is at least C^2], $\mathbf{\Delta v}(t)$ is at least C^1, and thus the relative velocity $\mathbf{\Delta v}(t_i)$ is also continuous at each node: $\mathbf{\Delta v}(t_i^+) = \mathbf{\Delta v}(t_i^-)$. Thus, $\mathbf{\Delta v}_i$ is sought to satisfy the defect $\boldsymbol{\xi}_i$:

$$\begin{cases} \mathbf{\Delta v}(t_i) = \mathbf{\Delta v}_i \\ \frac{\mathrm{d}\mathbf{\Delta v}}{\mathrm{d}t} = -\mu_{sun}\left(\frac{\mathbf{\Delta r}(t)+\mathbf{r}_{ast}(t)}{\|\mathbf{\Delta r}(t)+\mathbf{r}_{ast}(t)\|^3} - \frac{\mathbf{r}_{ast}(t)}{\|\mathbf{r}_{ast}(t)\|^3}\right) \\ \boldsymbol{\xi}_i = \mathbf{\Delta r}(t_{i+1}) - \mathbf{\Delta r}(t_i) - \int_{t_i}^{t_{i+1}} \mathbf{\Delta v}(t)\,\mathrm{d}t \end{cases} \tag{21}$$

These problems are boundary-value problems that are readily solved numerically by a shooting algorithm [20] or by a multiple-shooting method to solve all the $\Delta\boldsymbol{\xi}_i$ at once [21].

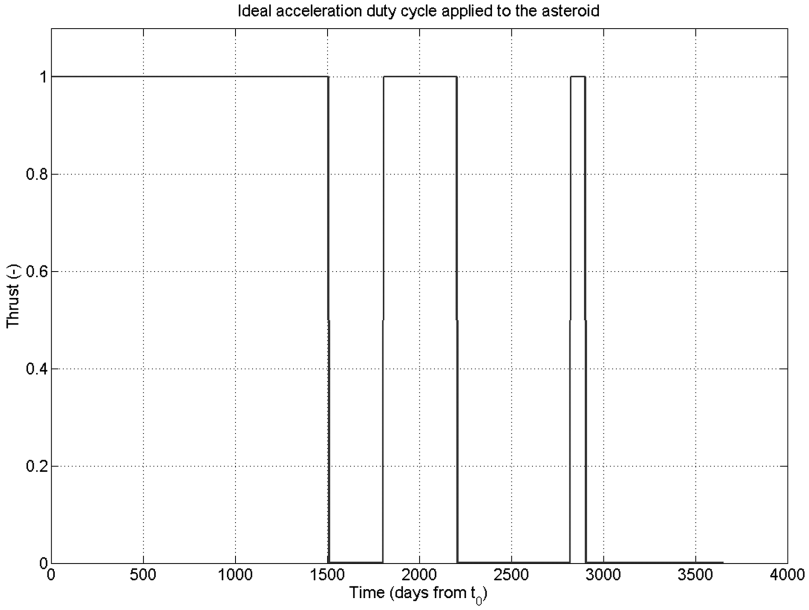

Fig. 6 Asteroid optimal deflection phases (control amplitude u_A).

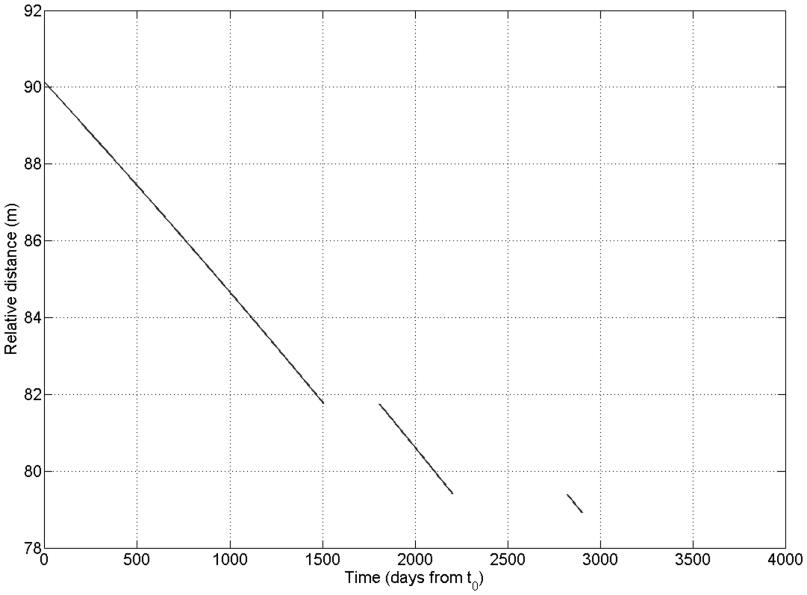

Fig. 7 Spacecraft relative distance during the towing phases. When the spacecraft is not thrusting, phases are left blank.

B. Spacecraft Trajectory During Nontowing Phases

1. *Possible Strategies*

During nontugging phases, the dynamic interaction between the spacecraft and the asteroid is limited to the mutual gravitation. According to Eq. (19), the spacecraft must be at infinite relative distance from the asteroid when not tugging. Placing the spacecraft at an infinite distance from the asteroid is equivalent to placing the spacecraft at a relative distance

$$d_{\mathrm{SOI}} = a\left(\frac{\mu_{\mathrm{ast}}}{\mu_{\mathrm{sun}}}\right)^{2/5} \tag{22}$$

which corresponds to the asteroid sphere of influence (SOI) radius [22]. Then the spacecraft has to perform escaping maneuvers. This analysis comes from the equilibrium relation equation (3); however, a close look at the dynamics gives us another option. Indeed, if the spacecraft simply stops thrusting and is placed on an orbit around the asteroid, the tugging effect does not exist either.

Because of the dynamics and the very small relative velocity of the asteroid, if the spacecraft stops thrusting, it would be on a highly eccentric orbit around the asteroid and would simply crash onto it. The spacecraft has to increase its thrust level T, either with additional thrusters or by reducing the cant angle ϕ toward zero, and correct its current orbit eccentricity.

2. *Dynamics*

The asteroid is assumed to be a homogeneous sphere. More complex shapes will be considered in future work, although some information can be found in the work of Kawaguchi et al. [23] for the Japan Aerospace Exploration Agency mission Hayabusa.

As in [4,5], the dynamic equation (4) is used. For simplification, $\mu_{\mathrm{ast}} \ll \mu_{\mathrm{sun}}$ is assumed, and since the spacecraft is evolving in the sphere of influence of the asteroid, the term relative to the sun gravitational acceleration can be neglected.

3. *Solution Method*

As a strategy, the spacecraft goes in minimum time on a circular parking orbit of radius d_{ref} around the asteroid and then goes back in minimum time into a hovering state. Consider t_1 and t_2 (respectively,

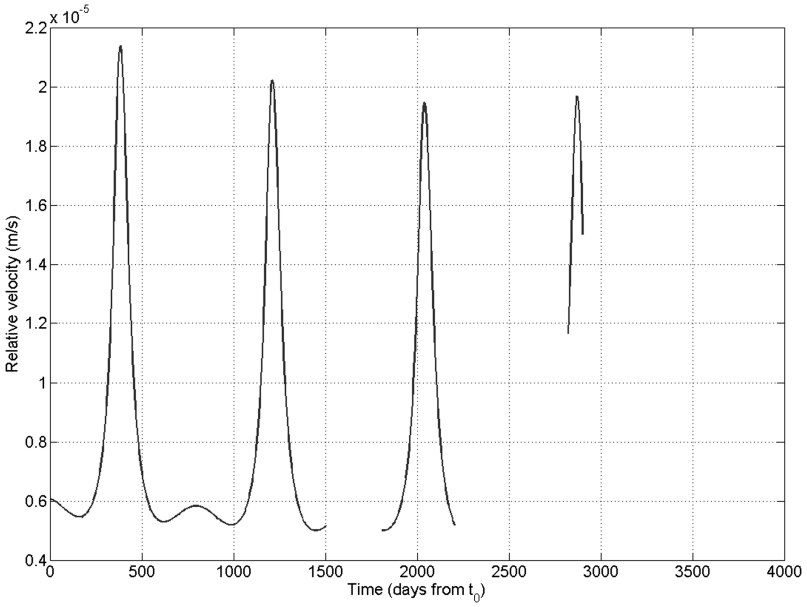

Fig. 8 Spacecraft relative velocity during the towing phases. When the spacecraft is not thrusting, phases are left blank.

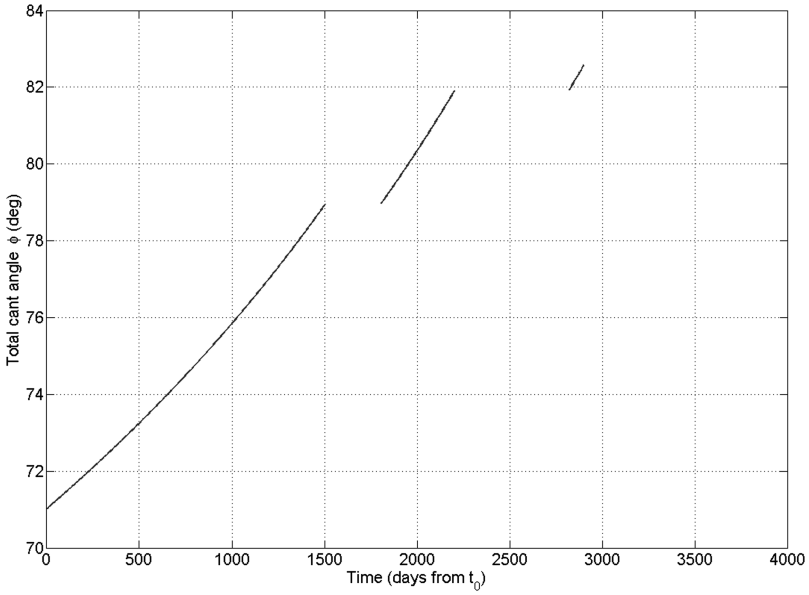

Fig. 9 Spacecraft thrust cant angle during the towing phases. When the spacecraft is not thrusting, phases are left blank.

the start and the end of the nontowing phase) and t_1^i and t_2^i (respectively, the dates when the spacecraft reaches and leaves, the circular orbit). Variables t_1 and t_2 are given, whereas t_1^i, and t_2^i are free parameters because of the minimum-time problems. The constraints for the intermediate states at t_1^i and t_2^i are given by

$$\|\Delta\mathbf{r}(t_1^i)\| - d_{\text{ref}} = 0 \tag{23}$$

$$E + \frac{\mu}{2d_{\text{ref}}} = 0 \tag{24}$$

$$\Delta\mathbf{r}\,(t_1^i)^T \Delta\mathbf{v}(t_1^i) = 0 \tag{25}$$

with the energy of the osculating orbit defined as

$$E = \frac{\|\Delta\mathbf{v}(t_1^i)\|^2}{2} - \frac{\mu_{\text{ast}}}{\|\Delta\mathbf{r}(t_1^i)\|}$$

and for the terminal state,

$$\Delta\mathbf{r}\,(t_2) = \Delta\mathbf{r}_2 \tag{26}$$

$$\Delta\mathbf{v}\,(t_2) = \Delta\mathbf{v}_2 \tag{27}$$

The first constraint imposes the point of injection at a given distance d_{ref}, the second constraint forces the energy to be that of an elliptic orbit of semimajor axis d_{ref}, and the third constraint imposes the circularity of the orbit. The last two constraints determine the state of the spacecraft for hovering. This state $[\Delta r_2, \Delta v_2]$ is determined by means of the inversion method described in Sec. IV.A. The state of the spacecraft at t_2^i is readily available because the spacecraft is on the circular orbit between t_1^i and t_2^i.

An equivalent problem can be formulated when the spacecraft goes back to the thrusting deflection state. The spacecraft on its circular orbit must reach a given state near the asteroid.

An optimal control problem is solved by the formulation of two separate TPBVPs. The optimality conditions are given by

$$\frac{\mathrm{d}\boldsymbol{\lambda}^T}{\mathrm{d}t} = -\boldsymbol{\lambda}^T \frac{\partial \mathbf{f}_s}{\partial \mathbf{x}} \tag{28}$$

$$\mathbf{u} = -\frac{\boldsymbol{\lambda}_{\mathbf{v}}}{\|\boldsymbol{\lambda}_{\mathbf{v}}\|} \tag{29}$$

and the transversality conditions for each problem are given by

$$[\boldsymbol{\lambda}_{\mathbf{r}}^T(t_1^i), \boldsymbol{\lambda}_{\mathbf{v}}^T(t_1^i)]^T = \nu_1 \frac{\partial E}{\partial[\Delta\mathbf{r}, \Delta\mathbf{v}]} + \nu_2 \frac{\partial\|\Delta\mathbf{r}\|}{\partial[\Delta\mathbf{r}, \Delta\mathbf{v}]} + \nu_3 \frac{\partial \Delta\mathbf{r}^T \Delta\mathbf{v}}{\partial[\Delta\mathbf{r}, \Delta\mathbf{v}]} \tag{30}$$

$$-H(t_1^i) = 1 + \nu_1 \frac{\partial E}{\partial t_1} + \nu_2 \frac{\partial\|\Delta\mathbf{r}\|}{\partial t_1} + \nu_3 \frac{\partial \Delta\mathbf{r}^{\mathrm{T}} \Delta\mathbf{v}}{t_1} \tag{31}$$

with ν_1, ν_2, and ν_3 Lagrange scalars assigned to the constraints, and

$$H(t_2^i) = 1 \tag{32}$$

The problem is solved using optimal control and a shooting method.

The spacecraft would need to thrust to change its velocity. Despite an almost null initial relative velocity, the velocity change required to reach such an orbit is likely to be very small because of the small gravitational constant of the asteroid.

It is likely, however, that performing the change of orbit can be more efficiently achieved by the use of chemical thrusters. The velocity change is so small, however, that having another propulsion system on board might not be interesting from a design point of view.

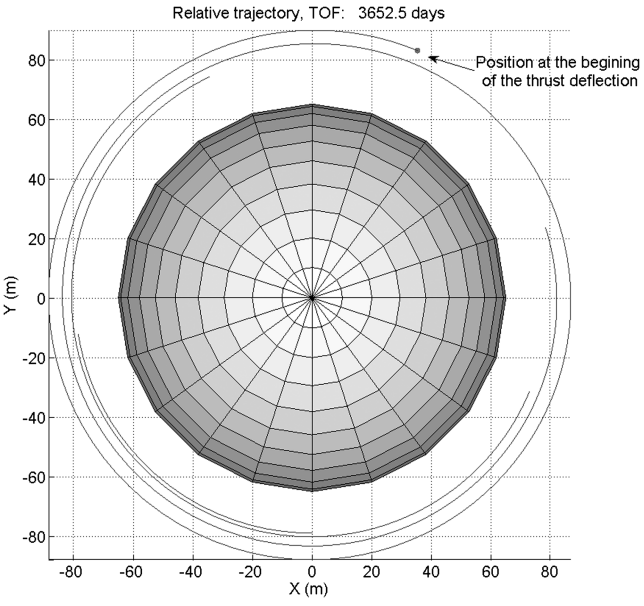

Fig. 10 Spacecraft trajectory in the asteroid frame during towing phases.

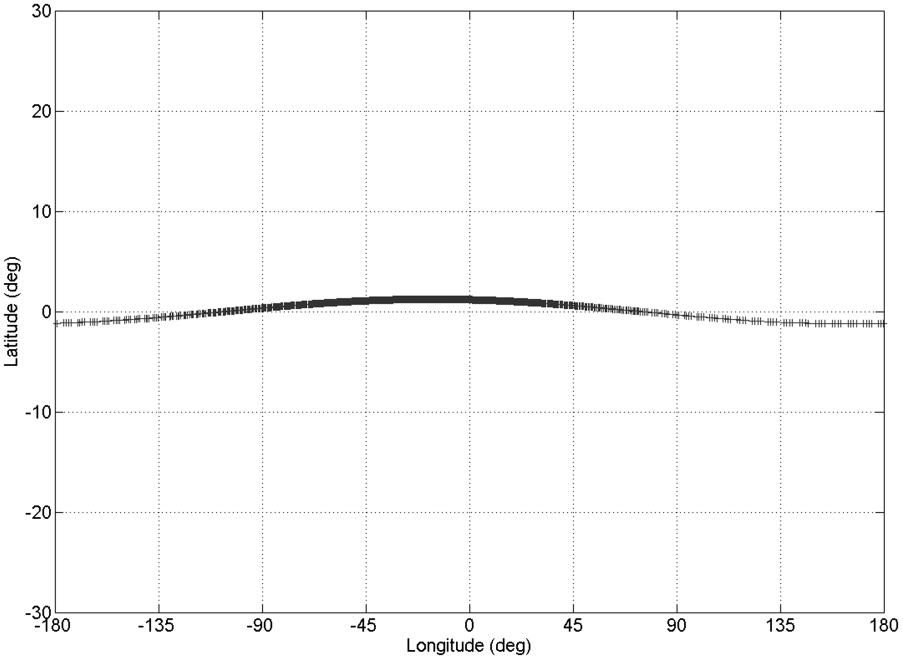

Fig. 11 Spacecraft latitude and longitude in the asteroid inertial reference frame.

V. Application: Optimal Deflection of 2007 VK184

The approach is applied to the deflection of asteroid 2007 VK184. This asteroid belongs to the Apollo family and is thus an Earth crossing near-Earth object. It has been selected because it currently belongs to the set of asteroids [24] graded 1 or higher on the Torino scale [25] with a nonzero impact probability. Grade 1 on the Torino scale basically means that careful attention is needed, as an impact is possible. This asteroid may eventually be downgraded to level zero (no risk) when further observations are available. Our choice is more academic and is not supposed to represent any future mission. Table 1 gives the main properties of the asteroid,[†] such as its orbit around the sun at the given epoch, and its mass.

The spacecraft is equipped with two NSTAR Xenon engines, with a specific impulse I_{sp} ranging from 1900 to 3100 s and a thrust force F_{th} from 92 to 19 mN for the lowest input power. To have an equilibrium distance of 90 m and $\phi = 66$ deg, the thrust force for each thruster should be 50 mN. If $I_{sp} = 2500$ s, the initial spacecraft wet mass is $m_0 = 1500$ kg and the spacecraft dry mass is $m_f = 800$ kg. The initial mass and the dry mass are chosen so that the cumulated thrust time does not exceed six years (it is currently the longest-duration experiment to date with an ion engine [19]), although the mission itself can exceed this duration. The date and time are explained in Table 2. The mission start date is deduced from the potential impact date and the warning time.

Figures 3 and 4 depict the difference in deflection between the fully thrusting deflection scenario and the optimal thrusting deflection scenario. Data for the fully thrusting deflection scenarios were computed from the work of Izzo [11]. When the time of flight to the potential impact date was too short to spend all the fuel, the fully thrusting strategy was chosen for both scenarios. Figure 3 depicts the deflection achieved for every encounter date. The shorter the remaining time to an encounter, the less the achieved deflection, in accordance with the results in [11].

Figure 4 shows the difference in deflection between the optimal deflection and the fully thrusting deflection. The difference in the deflection between the two strategies reaches about 100 km (about 6% of relative deflection magnitude) if the spacecraft starts deflecting the asteroid 10 years before the foreseen impact date. This difference might not be important, although in the worst case, the performance achieved is equal to the one obtained in the fully thrusting case, but including coast phases, which can be used for any operational concerns. For prekeyhole deflection, an order of magnitude of 100 km on the deflection is often sufficient. Some points toward the end of the graph either did not converge or the difference was extremely small and tolerance was not tight enough to improve it. So there are no improvements toward the end of the graph, despite the general trend of the oscillations. The difference can be much higher for asteroids with an initial high-eccentricity orbit. The curves are oscillating with a pseudoperiod, which is about one asteroid orbital period (828 days). The modulation is due to the term $(t_s - t)$ in Eq. (1).

For the sake of illustration, the point that presents 100 km in deflection is selected. Figure 5 plots the trajectory of the asteroid being deflected.

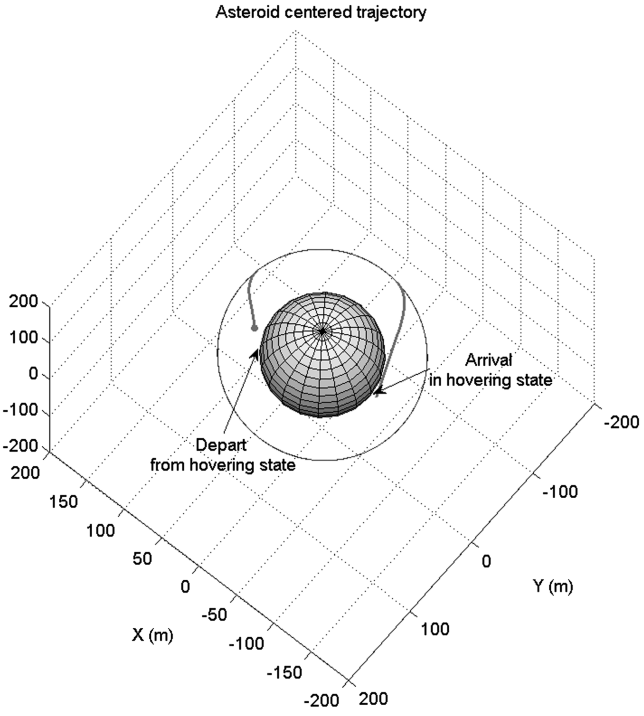

Fig. 12 Spacecraft trajectory in the asteroid frame during nontowing phases.

[†]Data available online at http://neo.jpl.nasa.gov/risk/2007vk184.html [retrieved 11 Jan. 2010].

Table 3 State at the beginning and end of the first non-thrust-deflecting phase, computed by the inversion dynamic method

	First nontowing phase	
Dates (from t_0)	1508.5 days	1804.3 days
Position $\Delta\mathbf{r}$, m	[72.596 21.997 1.36]	[−31.823 68.841 −1.057]
Velocity $\Delta\mathbf{v}$ (10^{-5} m/s)	[−0.137 0.459 0]	[−0.416 −0.209 −0.017]
Mass m_{sc}	969.6 kg	

Figure 5 depicts the deflected and nondeflected asteroid trajectories, and the deflection is so small that the difference in position is not visible at this scale. The arrows represent the direction of the perturbative acceleration induced by the gravity tractor. This direction is mostly tangential to the orbit, or parallel to the velocity vector, in accordance with Eq. (17). In fact, far from the potential impact date t_s, the perturbative acceleration induced by the spacecraft is collinear to the system's heliocentric velocity. The amplitude of the perturbation control $\mathbf{u}_A$ is plotted in Fig. 6; it shows three coast phases and three thrust phases.

Figures 7–9 depict the relative distance between the spacecraft and the asteroid, the relative velocity, and the cant angle. Clearly, because of the hovering, the relative velocity is small and almost zero. The cant-angle graph shows that when the spacecraft gets closer to the asteroid surface, the cant angle widens.

Figure 10 shows the equivalent relative trajectory. The distance variations come from the loss in mass during thrusting, making the equilibrium distance decrease. Even though the trajectory makes many revolutions around the asteroid, this motion is actually a slow motion, where the period is about one sidereal period of the asteroid around the sun.

Figure 11 shows that the spacecraft stays relatively close to the asteroid orbital plane. This means that the mutual acceleration does not go out of the ecliptic plane for this case, which is in accordance with the optimization.

Figure 12 describes the maneuver for an a orbit of 110 m of radius from the hovering position and the maneuver for going from the circular orbit to the new hovering position. Table 3 summarizes the boundary conditions. In contrast with Fig. 10, the motion is a rapid motion, where the period is the orbital period around the asteroid (41 min). The total transfer time is sufficiently small to not significantly change the mass budget of the spacecraft.

VI. Conclusions

A two-stage method to compute the gravity-tractor trajectory and optimal control deflection of an asteroid is presented. Simplified dynamic models of the asteroid and the spacecraft are used for towing and nontowing phases. The solar radiation pressure is neglected, and the asteroid is assumed to be a homogeneous sphere. The common assumption whereby an asteroid is continuously towed by the gravity tractor is discussed and determined to be nonoptimal. Optimal coast phases can provide slight improvements in the deflection.

The difference in scale between the spacecraft dynamics around the asteroid and the asteroid dynamics around the sun requires good precision. The method allows both dynamics to be independently computed. Therefore, since the computation of the deflection achieved is insensitive to the spacecraft dynamics, numerical calculations are accurate and reliable.

In the application case, the deflection of a near-Earth object is considered. The optimal deflection improves the nonoptimal deflection by a few hundred kilometers, which is sufficient for prekeyhole deflection. It is very likely that the difference between optimal and fully thrusting deflection is higher for asteroids with highly eccentric orbits. Furthermore, the control includes coast periods, which, from an operational point of view, allows time for recovering for any operational failures. Thus, the optimal deflection of an asteroid allows an improvement in both the deflection and the robustness.

References

[1] Ahrens, T., and Harris, A., "Deflection and Fragmentation of Near-Earth Asteroids," *Nature*, Vol. 360, No. 6403, 1992, pp. 429–433. doi:10.1038/360429a0

[2] Lu, E., and Love, S., "Gravitational Tractor for Towing Asteroids," *Nature*, Vol. 438, No. 7065, 2005, pp. 177–178. doi:10.1038/438177a

[3] Fahnestock, E., and Scheeres, D., "Dynamical Characterization and Stabilization of Large Gravity-Tractor Designs," *Journal of Guidance, Control, and Dynamics*, Vol. 31, No. 3, 2008, pp. 501–521. doi:10.2514/1.32554

[4] Wie, B., "Dynamics and Control of Gravity Tractor Spacecraft for Asteroid Detection," *Journal of Guidance, Control, and Dynamics*, Vol. 31, No. 5, 2008, pp. 1413–1423. doi:10.2514/1.32735

[5] McInnes, C., "Near Earth Object Orbit Modification Using Gravitational Coupling," *Journal of Guidance, Control, and Dynamics*, Vol. 30, No. 3, 2007, pp. 870–873. doi:10.2514/1.25864

[6] Broschart, S., and Scheeres, D., "Control of Hovering Spacecraft Near Small Bodies: Application to Asteroid 25143 Itokawa," *Journal of Guidance, Control, and Dynamics*, Vol. 28, No. 2, 2005, pp. 343–354. doi:10.2514/1.3890

[7] Gehler, M., Ober-Blobaum, S., Dachwald, B., and Marsden, J., "Optimal Control of Gravity Tractor Spacecraft Near Arbitrarily Shaped Asteroids," *1st IAA Planetary Defense Conference*, Granada, Spain, 27–30 April 2009.

[8] Izzo, D., Olympio, J., and Yam, C., "Asteroid Deflection Theory: Fundamentals of Orbital Mechanics and Optimal Control," *1st IAA Planetary Defense Conference*, Granada, Spain, 27–30 April 2009.

[9] Valsecchi, G. B., Milani, A., Gronchi, G. F., and Chesley, S. R., "Resonant Returns to Close Approaches: Analytical Theory," *Astronomy and Astrophysics*, Vol. 408, No. 3, 2003, pp. 1179–1196. doi:10.1051/0004-6361:20031039

[10] Yeomans, D., Bhaskaran, S., Broschart, S., Chesley, S., Chodas P., Jones, M., and Sweetser, T., "Near-Earth Object (NEO) Analysis of Transponder Tracking and Gravity Tractor Performance," Jet Propulsion Lab., California Inst. of Technology, Task Plan No. 82-120022, Pasadena, CA, Sept. 2008.

[11] Izzo, D., "Optimization of Interplanetary Trajectories for Impulsive and Continuous Asteroid Deflection," *Journal of Guidance, Control, and Dynamics*, Vol. 30, No. 2, 2007, pp. 401–408. doi:10.2514/1.21685

[12] Schweickart, R., Chapman, C., Durda, D., and Hut, P., "Threat Mitigation: The Gravity Tractor," B612 Foundation, White Paper 042, Sonoma, CA, June 2006

[13] Sanchez, P., Colombo, C., Vasile, M., and Radice, G., "Multicriteria Comparison Among Several Mitigation Strategies for Dangerous Near-Earth Objects," *Journal of Guidance, Control, and Dynamics*, Vol. 32, No. 1, 2009, pp. 121–142. doi:10.2514/1.36774

[14] Tschauner, J., and Hempel, P., "Rendezvous with a Target in Elliptic Orbit," *Astronautica Acta*, Vol. 11, No. 5, 1965, pp. 104–109.

[15] Betts, J., "Survey of Numerical Methods for Trajectory Optimization," *Journal of Guidance, Control, and Dynamics*, Vol. 21, No. 2, 1998, pp. 193–207. doi:10.2514/2.4231

[16] Broschart, S., and Scheeres, D., "Boundedness of Spacecraft Hovering Under Dead-Band Control in Time-Invariant Systems," *Journal of Guidance, Control, and Dynamics*, Vol. 30, No. 2, 2007, pp. 601–610. doi:10.2514/1.20179

[17] Pontryagin, L. S., Boltyanskii, V. G., Gamkrelidze, R. V., and Mishchenko, E., *The Mathematical Theory of Optimal Processes*, Interscience Publishers, New York, 1962, Chap. 1.

[18] Bertrand, R., and Epenoy, R., "New Smoothing Techniques for Solving Bang-Bang Optimal Control Problems—Numerical Results and Statistical Interpretation," *Optimal Control Applications and Methods*,

Vol. 23, No. 4, 2002, pp. 171–197.
doi:10.1002/oca.709

[19] Rayman, M., Fraschetti, T., Raymond, C., and Russell, T., "Dawn: A Mission in Development for Exploration of Main Belt Asteroids Vesta and Ceres," *Acta Astronautica*, Vol. 58, No. 11, 2006, pp. 605–616.
doi:10.1016/j.actaastro.2006.01.014

[20] Keller, H., *Numerical Methods for Two-Point Boundary-Value Problems*, Dover, New York, 1992, pp. 7–18.

[21] Kierzenka, J., and Shampine, L., "A BVP Solver Based on Residual Control and the MATLAB PSE," *ACM Transactions on Mathematical Software*, Vol. 27, No. 3, 2001, pp. 299–316.
doi:10.1145/502800.502801

[22] Battin, R., *An Introduction to the Mathematics and Methods of Astrodynamics*, Rev. ed., AIAA Education Series, AIAA, Reston, VA, 1999.

[23] Kawaguchi, J., Fujiwara, A., and Uesugi, T., "Hayabusa—Its Technology and Science Accomplishment Summary and Hayabusa-2," *Acta Astronautica*, Vol. 62, Nos. 10–11, 2008, pp. 639–647.
doi:10.1016/j.actaastro.2008.01.028

[24] Yeomans, D., and Baalke, R., "Sentry Risk Table," May 2009, http://neo.jpl.nasa.gov/risks/index.html [retrieved 11 Jan. 2010].

[25] Binzel, R. P., "The Torino Impact Hazard Scale," *Planetary and Space Science*, Vol. 48, No. 4, 2000, pp. 297–303.
doi:10.1016/S0032-0633(00)00006-4